Modelling of Brain Consciousness based on Collaborative Adaptive Filters

Ling Li[a,*], Yili Xia[a], Beth Jelfs[a], Jianting Cao[b,c,d], Danilo P. Mandic[a]

[a]*Department of Electrical and Electronic Engineering, Imperial College London, SW7 2BT, UK*
[b]*Department of Electronic Engineering, Saitama Institute of Technology, Japan*
[c]*Laboratory for Advanced Brain Signal Processing, RIKEN Brain Science Institute, Saitama 351-0198, Japan*
[d]*East China University of Science and Technology, Shanghai, 200237*

Abstract

A novel method for the discrimination between discrete states of brain consciousness is proposed, achieved through examination of nonlinear features within the electroencephalogram (EEG). To allow for real time modes of operation, a collaborative adaptive filtering architecture, using a convex combination of adaptive filters is implemented. The evolution of the mixing parameter within this structure is then used as an indication of the predominant nature of the EEG recordings. Simulations based upon a number of different filter combinations illustrate the suitability of this approach to differentiate between the coma and quasi-brain-death states based upon fundamental signal characteristics.

Keywords: Collaborative adaptive filtering, EEG, quasi-brain-death (QBD), coma, signal nonlinearity

1. Introduction

The investigation of the information processing mechanisms of the brain, including consciousness states, is an active area of research. When considering consciousness status the identification of brain death is an important topic within such research as there can be severe implications of declaring a

*Corresponding author.
Email address: Ling.Li206@imperial.ac.uk (Ling Li)

patient brain dead - the legal definition of brain death is "irreversible loss of forebrain and brainstem functions" [1]. However, different medical criteria for determining brain death have been established in the different countries [2]. One such diagnostic example is the Takeuchi criterion [3] which involves the following series of tests: coma test, pupil test, brainstem reflexes test, apnea test, and EEG confirmatory test [4]. As can be imagined, with such thorough testing, it can be difficult to implement brain death diagnosis effectively. Specialized personnel and technology are needed to perform a series of tests which are expensive, time consuming and can put patient at a risk.

Although the diagnostic criteria are different from country to country, in general these tests can put the patient at potential medical risk due to the requirements of implementing the tests. Namely brain death tests require that medical care instruments be removed (apnea test), whereas, some tests require that the patient be transported out of the intensive care unit (ICU). Other, confirmatory tests, can take as long as 30 minutes each and need to be performed several times over intervals of up to ten hours, these tests put stress on already compromised organs [5]. To overcome the above difficulties, a preliminary EEG test has been proposed in [6], to be used to determine whether further brain death tests, especially those requiring patients to be disconnected from important medical devices, need to be implemented, in this way an initial prognosis of quasi-brain-death (QBD) is given. The term "quasi-" means that this is a preliminary decision, because in this paper we are actually focusing on the situation that the brain death diagnosis was made at an early stage, which was judged independently by two medical doctors or physicians, whereas the final diagnosis of brain death needs further medical tests (apnea test, EEG confirmatory test).

There are various methods for EEG based analysis of brain states [7, 8], typical tools include phase synchrony [9, 10], coherence [11], and nonlinear dynamical analysis [12, 13]. This research suggests that tracking the dynamics of nonlinear characteristics within the signals is a key for analyzing EEG signals [4]. It is further argued in [4, 13] that the assessment of the nonlinear nature of EEG signals can provide a platform for the identification of the brain consciousness states.

One method for performing the assessment of nonlinearity within a signal in real time is through the use of collaborative adaptive filters. Collaborative adaptive filters were originally introduced as a method of achieving quantitative improvement in performance, and the stability analysis can be found in [14]. However, recently it has been shown that by tracking the adaptive

mixing parameter within such a structure it is possible to gain an indication of which subfilter within the structure currently has the better performance in term of their prediction errors. As the two subfilters within the collaborative hybrid filter structure operate in parallel, by appropriate selection of their training algorithms, the resulting parameterized feature maps, can be used to gain an insight into the underlying nature of the input signal. Thus, this technique provides a convenient, flexible method which can test for fundamental signal properties [15]. From the medical viewpoint, such filters offer real time processing ability and hence reduce the risk to the patient when performing QBD tests. Unlike hypothesis testing based methods [13], which are block-based, such as the Delay Vector Variance (DVV) [16], this approach also performs testing for the degree of nonlinearity in nonstationary environments.

In this work, we focus on the role of the degree of nonlinearity in identification of different states of brain consciousness (awake, coma, QBD). First we present the hybrid filter structure for collaborative adaptive filtering and evaluate the usefulness of this approach on synthetic benchmark linear and nonlinear signals. It is then illustrated that such an approach can discriminate between awake, coma and quasi-brain-death states from real world EEG signals. In order to provide a more complete understanding of the nature of the EEG signals, a general test for nonlinearity is presented. Following this we then consider sparsity as a type of nonlinearity and the combination of both of these tests to give an enhanced nonlinear feature map. Finally, a potential solution in the complex domain to the signal modality characterisation is considered. Complex signals can be either complex by design or by convenience of representation, and one such representation is to use pairs of electrodes to form a complex variable. Such representations have been shown to provide more degrees of freedom [17, 18], and in the complex domain, we consider the complex noncircularity of the EEG data.

2. The Hybrid Filtering Architecture

Collaborative adaptive filtering refers to an architecture in which adaptive filters operate in parallel and feed into a mixing algorithm to produce the single output of the filter [14]. One simple form of mixing algorithm is a convex combination of two filters in which the mixing parameter $\lambda(k)$ adaptively combines the outputs of each subfilter as shown in Fig. 1. The overall filter output $y(k)$ is the convex combination of the outputs of the subfilters

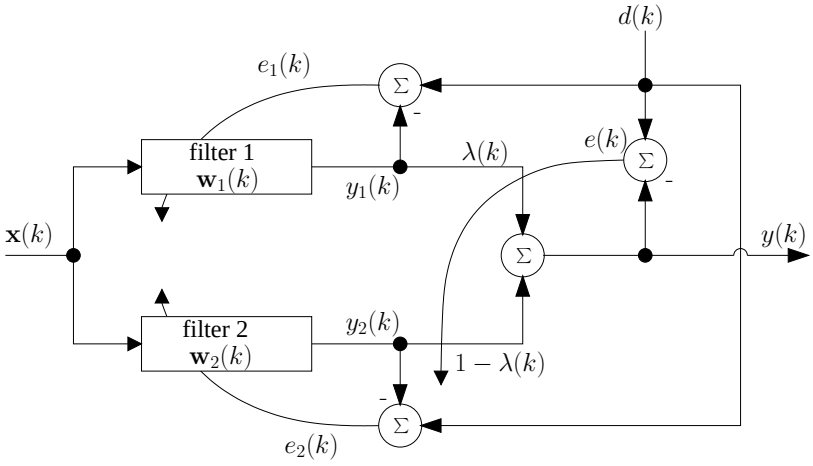

Figure 1: Hybrid combination of two adaptive subfilters.

given by

$$y(k) = \lambda(k)y_1(k) + (1 - \lambda(k))y_2(k), \tag{1}$$

where $y_1(k)$ and $y_2(k)$ are the outputs of the constituent subfilters. The mixing parameter $\lambda(k)$ is updated based on minimization of the quadratic cost function of the instantaneous filter error $\mathcal{J}(k) = e^2(k)$. The update can be obtained using the following gradient descent adaptation

$$\lambda(k+1) = \lambda(k) - \mu_\lambda \nabla_\lambda \mathcal{J}(k)_{|\lambda=\lambda(k)}, \tag{2}$$

where μ_λ is the adaptation step-size. The update of $\lambda(k)$, allowing for possible complex inputs and thus complex errors, can be obtained as [15]

$$\begin{aligned}
\lambda(k+1) =& \lambda(k) - \mu_\lambda \left[e(k) \frac{\partial e^*(k)}{\partial \lambda(k)} + e^*(k) \frac{\partial e(k)}{\partial \lambda(k)} \right] \\
=& \lambda(k) + \mu_\lambda \left[e(k) \big(y_1(k) - y_2(k) \big)^* + e^*(k) \big(y_1(k) - y_2(k) \big) \right] \\
=& \lambda(k) + \mu_\lambda \Re \left[e(k) \big(y_1(k) - y_2(k) \big)^* \right].
\end{aligned} \tag{3}$$

where $\Re[\cdot]$ denotes the real part of a complex number.

Originally, the applications of hybrid filters focused mainly on the improvement in the performance over the individual constituent filters. However, recent research has shown that by appropriate selection of the subfilters,

the evolution of the mixing parameter $\lambda(k)$ can give an instantaneous indication of fundamental characteristics of the input signal [4, 15]. Our aim is to discriminate between brain states based on the fundamental signal characteristics of the EEG, and as such the algorithm used to train the subfilters are selected based on their ability to process signals with the characteristics of interest. First we shall consider a test for the presence of nonlinearity in a signal and illustrate the application of this method with an example on benchmark synthetic data. Having illustrated the applicability of this test, we will then outline the algorithms used for assessing different signal characteristics.

2.1. Collaborative Adaptive Filtering for the Identification & Tracking of Nonlinearity

The collaborative adaptive filter for identification of nonlinearity compromises a linear FIR adaptive subfilter trained by the least mean square (LMS) algorithm [19] and a nonlinear FIR subfilter trained by the normalized nonlinear gradient descent (NNGD) algorithm [20]. The output of subfilter *Filter* 1 trained by the LMS algorithm is generated as

$$\begin{aligned} y_{LMS}(k) =& \mathbf{x}^T(k)\mathbf{w}_{LMS}(k), \\ e_{LMS}(k) =& d(k) - y_{LMS}(k), \\ \mathbf{w}_{LMS}(k+1) =& \mathbf{w}_{LMS}(k) + \mu e_{LMS}(k)\mathbf{x}(k), \end{aligned} \tag{4}$$

and $y_{NNGD}(k)$ is the corresponding output of the NNGD trained subfilter *Filter* 2 given by [20]

$$\begin{aligned} net(k) =& \mathbf{x}^T(k)\mathbf{w}_{NNGD}(k), \\ y_{NNGD}(k) =& \Phi(net(k)), \\ e_{NNGD}(k) =& d(k) - y_{NNGD}(k), \\ \mathbf{w}_{NNGD}(k+1) =& \mathbf{w}_{NNGD}(k) + \eta(k)e_{NNGD}(k)\Phi'(net(k))\mathbf{x}(k), \\ \eta(k) =& \frac{\mu}{\left[\left(\Phi'(net(k))\right)^2 \|\mathbf{x}(k)\|_2^2\right] + C}, \end{aligned} \tag{5}$$

where $d(k)$ is the desired output, $\mathbf{x}(k) = [x(k-1), x(k-2), \ldots, x(k-N)]^T$ is the tap input vector, $\Phi(\cdot)$ is the nonlinear activation function, C is the regularization parameter and μ is the step-size for both algorithms. Each subfilter operate in a one step ahead prediction setting and are adapted

based on their own errors $e_{LMS}(k)$ and $e_{NNGD}(k)$ respectively to give the individual weight updates $\mathbf{w}_{LMS}(k)$ and $\mathbf{w}_{NNGD}(k)$.

To illustrate the effectiveness of the hybrid filter in tracking signal nonlinearity, synthetic inputs were formed by alternating nonlinear and linear signal segments. This gives the benchmark signal comprising the nonlinear signal [21]

$$z(k+1) = \frac{z(k)}{1+z^2(k)} + n^3(k), \tag{6}$$

and stable linear AR(4) process

$$r(k) = 1.79r(k-1) - 1.85r(k-2) + 1.27r(k-3) - 0.41r(k-4) + n(k), \tag{7}$$

where $n(k)$ is a zero mean, unit variance white Gaussian process. The signal comprised of 10000 samples alternating between processes every 1000 samples. In this case, we are not interested in the overall performance of the filter but in whether the dynamics of the mixing parameter $\lambda(k)$ can give an illustration of which subfilter is responding to the characteristics of the input signal most effectively. By design, the value of $\lambda(k)$ varies between 0 and 1, with 1 indicating strong linearity in signal nature and 0 a strong nonlinearity. The initial value of mixing parameter $\lambda(k)$ was set to 0.5, as there was no prior assumption of the signal linearity or nonlinearity. The simulation result shown in Fig. 2 presents the evolution of the mixing parameter $\lambda(k)$ on the prediction of the benchmark synthetic signal. As desired, the value of $\lambda(k)$ decreases towards 0.3 in the first 1000 samples, which correctly suggests the nonlinear nature of the signal described by (6). In contrast, for the AR(4) process (samples 1001:2000), $\lambda(k)$ increased towards 0.9 indicating the linear nature of the benchmark input signal described in (7). This suggests that the hybrid filter has great potential for tracking linear and nonlinear characteristics of real world signals.

2.1.1. Hybrid Filter for Identification of Sparsity

Before moving on to consider the EEG data we first outline the algorithms used to produce alternative hybrid filters for identification of different fundamental signal characteristics. As nonlinearity covers a wide range of signals the first characteristic we will consider is sparsity (a subset of nonlinearity), as sparse signals occur naturally in many real world applications. A sparse signal is one for which the impulse response of an unknown system has a large number of zero elements and only relatively few active ones. For

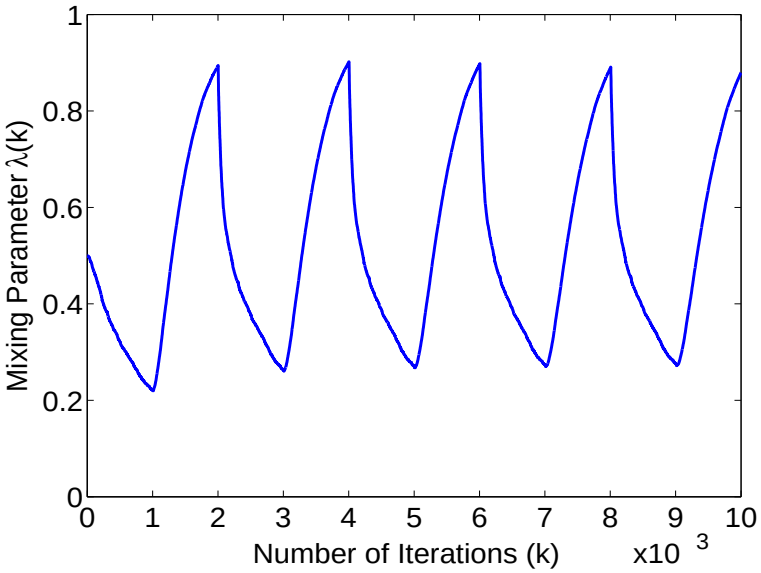

Figure 2: The evolution of the mixing parameter $\lambda(k)$ for a signal nature alternating between nonlinear to linear every 1000 samples.

the purpose of identifying the sparsity of a signal the algorithm used to train subfilter *Filter* 2 in the hybrid filter structure is replaced with the signed sparse LMS (SSLMS). The output of the SSLMS is given by [22]

$$\begin{aligned} y_{SSLMS}(k) =& \mathbf{x}^T(k)\mathbf{w}_{SSLMS}(k), \\ e_{SSLMS}(k) =& d(k) - y_{SSLMS}(k), \\ \mathbf{w}_{SSLMS}(k+1) =& \mathbf{w}_{SSLMS}(k) + \mu|\mathbf{w}(k) + \varepsilon|e_{LMS}(k)\mathbf{x}(k), \end{aligned} \tag{8}$$

where ε is a small positive constant used to prevent the update stalling for small values of $\mathbf{w}(k)$. The use of this algorithm within the hybrid filter structure has been shown to achieve good results when tracking changes in signal nature of EEG signals [15].

2.2. Collaborative Adaptive Filtering in the Complex Domain

The collaborative adaptive filtering for signal modality characterisation in the real domain $\mathbb{R}$ has been well-established. Recently, efforts have been made to achieve the on-line tracking of nonlinearity in the complex domain [15]. These extensions of hybrid filters from $\mathbb{R}$ to $\mathbb{C}$ are not trivial,

due to the fact that the nature of nonlinearity in $\mathbb{C}$ is fundamentally different from these in $\mathbb{R}$. In this paper, we focus on noncircularity, another key property when processing in $\mathbb{C}$.

2.2.1. Hybrid Filter for Identification of Complex Circularity

A circular signal is one with a rotation-invariant distribution and the second order statistics of a circular complex signal can be sufficiently represented using the standard complex covariance matrix $\mathcal{C}_{\mathbf{zz}} = E[\mathbf{z}\mathbf{z}^H]$, where $(\cdot)^H$ is the Hermitian transpose. However, circular data occurs only in a limited number of applications and to accurately model the generality of complex signals we need to take into account not only the standard covariance matrix but also the pseudocovariance matrix $\mathcal{P}_{\mathbf{zz}} = E[\mathbf{z}\mathbf{z}^T]$. To this end, so called augmented complex statistics allow for accurate modelling of both circular and noncircular signals by defining an augmented complex vector $\mathbf{z}_a$ as

$$\mathbf{z}_a = \begin{bmatrix} \mathbf{z} \\ \mathbf{z}^* \end{bmatrix}, \tag{9}$$

with the augmented covariance matrix given by [23]

$$\mathcal{R}_{\mathbf{zz}} = \begin{bmatrix} \mathcal{C}_{\mathbf{zz}} & \mathcal{P}_{\mathbf{zz}} \\ \mathcal{P}^*_{\mathbf{zz}} & \mathcal{C}^*_{\mathbf{zz}} \end{bmatrix}, \tag{10}$$

containing information from both the covariance and pseudocovariance matrices of $\mathbf{z}$. A second order circular signal is also termed proper and has a zero pseudocovariance matrix $\mathcal{P}_{\mathbf{zz}} = \mathbf{0}$ [24, 25].

The proposed approach for the assessment of signal noncircularity is based on a hybrid filter for complex data with a combination of the standard CLMS [26] (complex version of LMS) and augmented CLMS (ACLMS) algorithms [27, 28]. The filter update of the CLMS is given by [26]

$$\mathbf{w}_{CLMS}(k+1) = \mathbf{w}_{CLMS}(k) + \mu e_{CLMS}(k)\mathbf{x}^*(k), \tag{11}$$

The recently introduced ACLMS algorithm extends the CLMS algorithm to use augmented statistics and thereby utilise the full second order statistical information available within the signal. The ACLMS is given by

$$\begin{aligned} e_{ACLMS}(k) =& d(k) - y_{ACLMS}(k), \\ y_{ACLMS}(k) =& \mathbf{h}^T_{ACLMS}(k)\mathbf{z}(k) + \mathbf{g}^T_{ACLMS}(k)\mathbf{z}^*(k), \\ \mathbf{h}_{ACLMS}(k+1) =& \mathbf{h}_{ACLMS}(k) + \mu e_{ACLMS}(k)\mathbf{z}^*(k), \\ \mathbf{g}_{ACLMS}(k+1) =& \mathbf{g}_{ACLMS}(k) + \mu e_{ACLMS}(k)\mathbf{z}(k). \end{aligned} \tag{12}$$

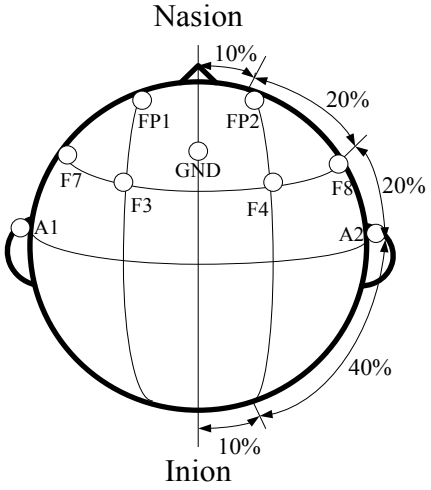

Figure 3: The Electrode placement.

However, the ACLMS results in a filter which is effectively twice the length of that of the CLMS, leading to the CLMS having a faster initial convergence rate than the ACLMS. Using a convex combination of these algorithms allows the hybrid filter to take advantage of both the improved performance of the ACLMS for filtering of noncircular signals, along with the faster convergence of the CLMS.

3. The EEG Data

The EEG data were recorded in the ICU in HuaShan Hospital, Shanghai, China. The room was quiet, but the surrounding noise generated by other monitoring machines was high. The recordings were taken with all the patients involved lying on bed face up with eyes closed. The data was obtained via nine electrodes on the forehead with channels based on the 10-20 system, the positions of these electrodes can be seen on Fig. 3. The electrodes were placed at positions F3, F4, F7, F8, Fp1, Fp2 as well as GND, and also two were placed on the ears (denoted by A1 and A2 respectively). The electrodes placed on the ears act as a reference for the measurements, calculated as (A1+A2)/2. The measured voltage signal was then digitized via a portable EEG recording instrument with a sampling frequency of 1kHz. Experimental data was obtained from 34 patients of ages ranging from 17 to 85 years old; half of the patients were in a state of coma, and the other

half had already been assessed to be in quasi-brain-death status by clinical doctors. Total EEG recordings from these 34 patients with an average length of five minutes were stored and analyzed. For the purpose of analysis only the first channel obtained from electrode Fp1 was used for real domain analysis and first and second channel obtained from electrodes Fp1 and Fp2 were used for the complex domain analysis. To obtain the complex valued signals it is natural to use a pair of electrodes symmetrically placed on the patient as such the electrodes Fp1 and Fp2 from Fig. 3. These were then made complex in the form Fp1 + $\jmath$Fp2.

4. Simulation Results

We shall now consider the use of hybrid filters for application on real world EEG signal for the purpose of brain consciousness state identification. The first set of simulations consider the use of the hybrid filter described in Section 2.1 for identification of nonlinearity. The step size used for the adaptation of was $\mu_\lambda = 0.01$ and the initial value of $\lambda(0) = 0.5$. The learning rate of the linear FIR adaptive subfilter was 0.002 and the learning rate of the nonlinear FIR subfilter trained by NNGD algorithm was 0.01. Results shown in Fig. 4, Fig. 5 and Fig. 6 present the examples of EEG signals for the states of 'awake', 'coma' and 'QBD', and the corresponding evolution of the mixing parameter $\lambda(k)$ for the different brain consciousness states.

Figure 4 shows the EEG data of a patient in an 'awake' state. The top plot presents the amplitude of the brain signal over 100 seconds. The evolution of the corresponding mixing parameter $\lambda(k)$ is shown in the bottom graph. It can be seen that the value of $\lambda(k)$ for the awake EEG data moves towards $\lambda = 1$ as the adaptation progresses. This suggest the linearity of the EEG signals of awake patients. Figure 5 presents the EEG signal of a 'coma' patient; the curve of $\lambda(k)$ gives no clear indication of signal nonlinearity. However, during the analysis of quasi-brain-death signals of the same time period (100 seconds) shown in Figure 6, the mixing parameter $\lambda(k)$ moved towards zero, indicating the nonlinear nature of the signal.

In order to have a general knowledge of the all available data, the average mixing parameter $\lambda(k)$, together with standard deviations for all 34 patients are shown in Fig. 7. The results of the coma patients are shown in black, and the 'QBD' patient results are shown in grey. The errorbars were plotted every 2000 iterations. It can be seen that the average response of $\lambda(k)$ for 'QBD' patients shows predominately nonlinear natures of the underlying signals,

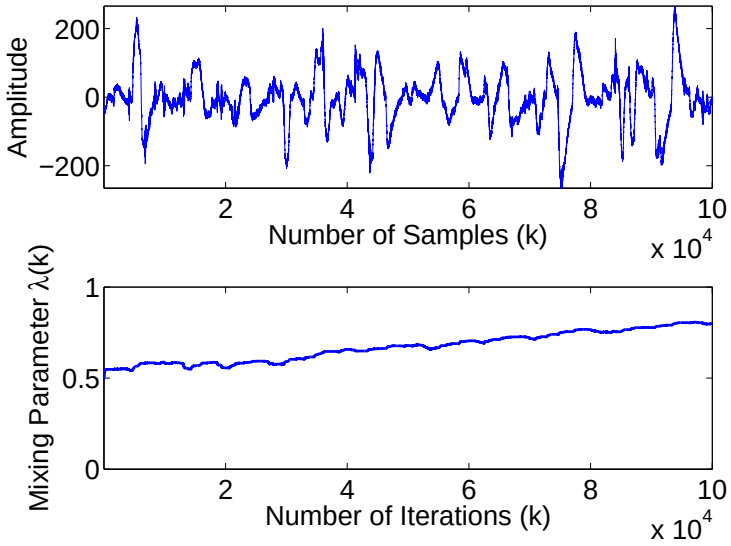

Figure 4: An example of the signal for an awake patient (top) and the dynamics of the mixing parameter $\lambda(k)$ of awake patient (bottom), $\lambda = 1$ corresponds to linear subfilter.

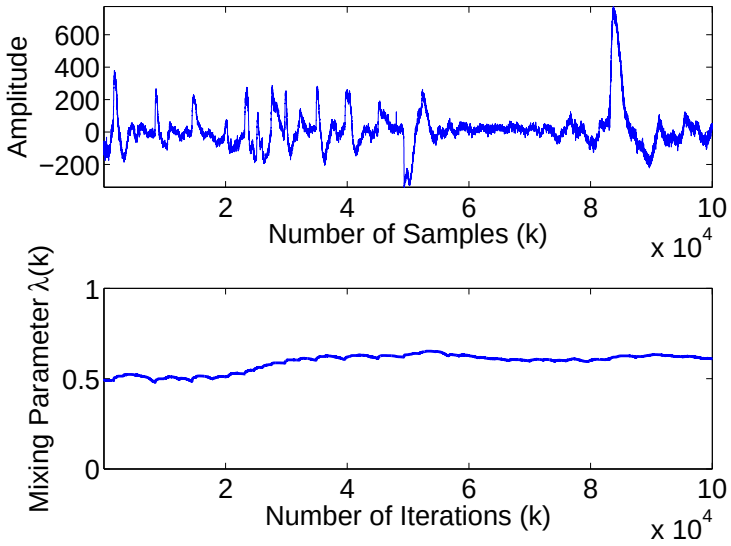

Figure 5: An example of the signal for a coma patient (top) and the dynamics of the mixing parameter $\lambda(k)$ of coma patient (bottom), $\lambda = 1$ corresponds to linear subfilter.

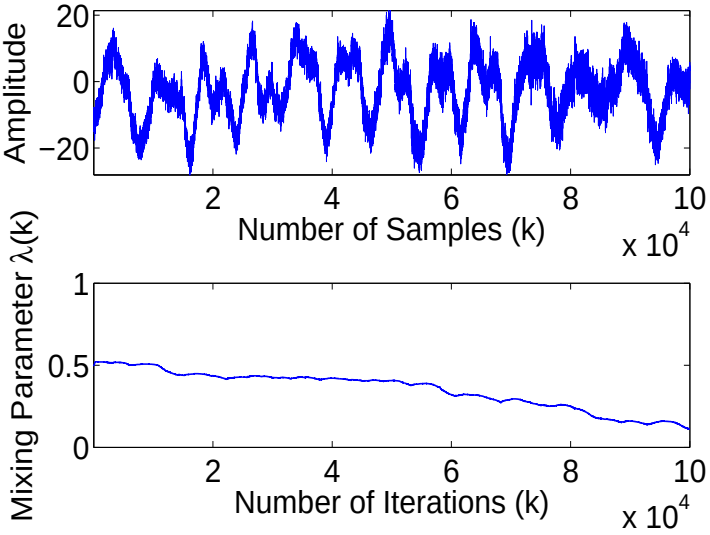

Figure 6: An example of the signal for a 'QBD' patient (top) and the dynamics of the mixing parameter $\lambda(k)$ of 'QBD' patient (bottom), $\lambda = 1$ corresponds to linear subfilter.

whereas, on the average, for the coma patients the results were not decisive with the value of $\lambda(k)$ around 0.5. The data was quite noisy and subject to artifacts and thus, for instance, when we used all the available data, the mean curves representing the evolution of the mixing parameter λ were quite far apart, but the error bars overlapped considerably, even after convergence. If, however, we include only the 30 least noisy recordings, eliminating two less noisiest recordings from each group. The results, as shown in Fig. 8, were greatly improved, where perfect identification of the QBD and coma patients was achieved after convergence.

To further evaluate the effectiveness of the analysis, the Support Vector Machine (SVM) classification method was applied using a Gaussian kernel. The SVM soft margin classifier used was a Quadratic Programming (QP) algorithm [29]. The conditioning parameter set for the QP algorithm was 0.000001. The sample vector used contained 5 columns which are obtained using Principal Components Analysis (PCA) [30] from the principal component space of all the available estimated λ. The classification accuracy and the standard deviation were evaluated on the average of 100 trials. The classification accuracy for 34, 32 and 30 patients as shown in Fig. 9, were 68.54%, 73.75% and 77.83%. It is worth noting that the results shown in

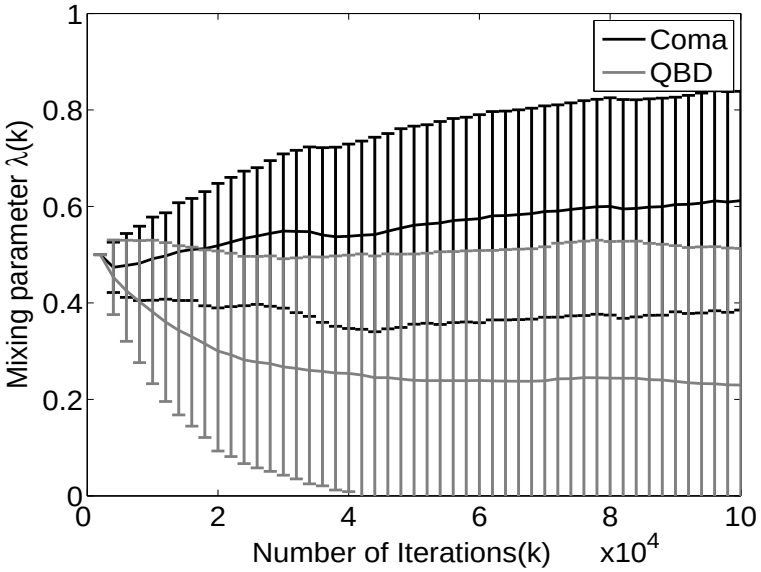

Figure 7: The evolution of the average mixing parameter $\lambda(k)$ for signal nonlinearity detection with corresponding standard deviation error bars for 17 coma patients, 17 'QBD' patients. $\lambda = 1$ corresponds to linear subfilter.

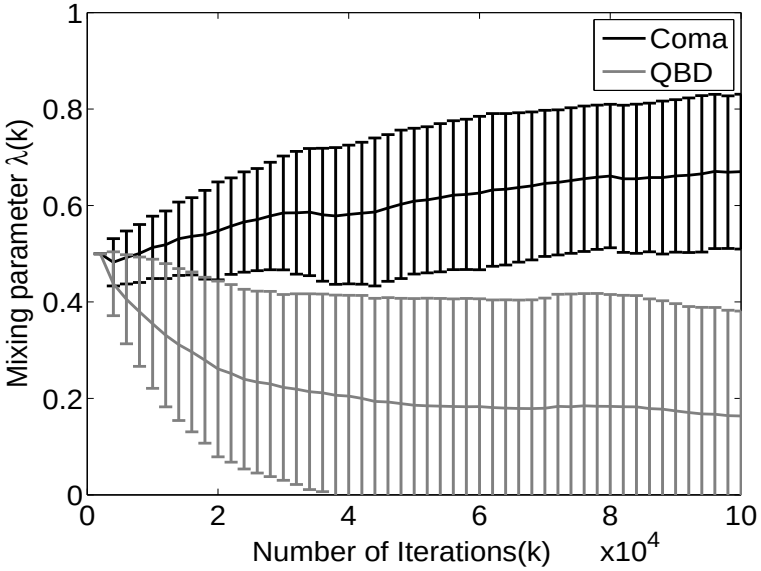

Figure 8: The evolution of the average mixing parameter $\lambda(k)$ for signal nonlinearity detection with corresponding standard deviation error bars for 15 coma patients, 15 QBD patients. $\lambda = 1$ corresponds to linear subfilter.

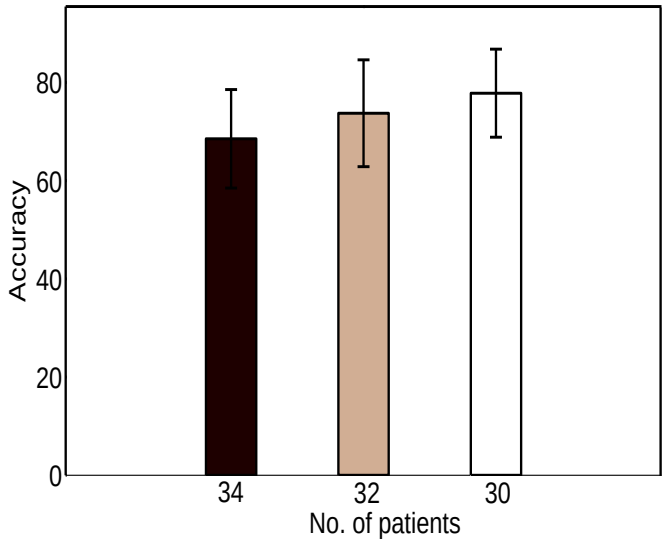

Figure 9: The accuracy of learning of collaborative adaptive filter using SVM.

Fig. 9 were obtained over the whole evolution of the mixing parameter λ; these classification results could, therefore, be increased by applying SVM to only the converged values of λ. The classification results further prove that analyzing the signal linearity of EEG data using the mixing parameter $\lambda(k)$ of a hybrid filter is an effective approach to identifying coma and QBD brain status.

Following the analysis of nonlinearity, it is natural to consider whether identifying specific types of nonlinearity improves the performance, particularly as the nonlinearity assessment of the coma patients was not decisive. To this end, sparsity analysis of the EEG data was performed using the hybrid filter described in Section 2.1.1. The step size used for the adaptation of λ was $\mu_\lambda = 0.068$ and the initial value of $\lambda(0) = 1$. The value of $\lambda = 1$ was chosen as we know the QBD patient signals are nonlinear in nature so starting from a linear assumption prevents the adaptation of λ from quickly stalling allowing us to better view the degree of signal sparsity. The learning rate of the linear FIR adaptive subfilter was 0.001 and the learning rate of the FIR subfilter trained by SSLMS algorithm was 0.006. Simulation results for 50 seconds of data for different numbers of patients are shown in Fig. 10 and Fig. 11. Results in Fig. 10 show the average mixing parameter $\lambda(k)$ with the standard deviation error bars for all 34 patients for the analysis

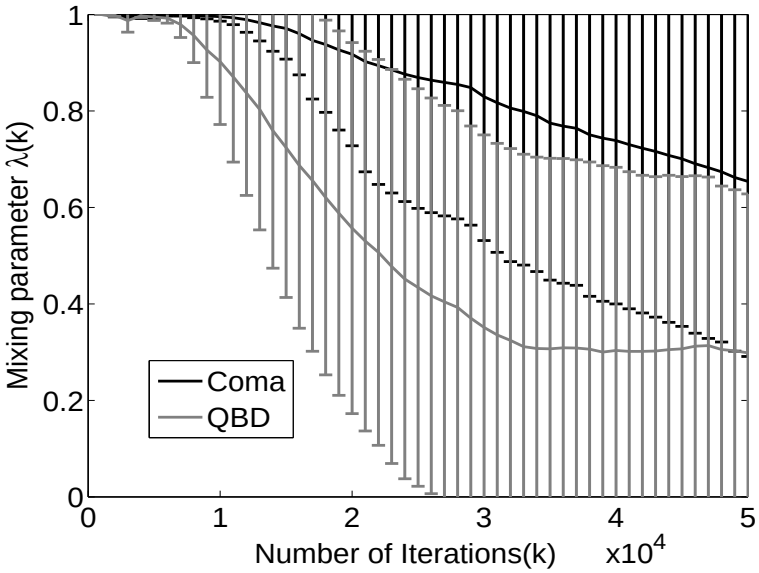

Figure 10: The evolution of the average mixing parameter $\lambda(k)$ for signal sparsity detection, for patients in different brain states, with corresponding standard deviation error bars for 17 coma patients, 17 QBD patients. $\lambda = 1$ corresponds to linear subfilter.

of signal sparsity. Similarly to the linearity analysis, the results for coma patients are shown in black and QBD analysis in grey, and the errorbars are shown every 2000 iterations. It can be seen that the average response of $\lambda(k)$ for QBD patients is approximately 0.3 whereas that of the coma patients is approximately 0.7. Figure 11 shows the analysis of the 15 pairs of least noisy recordings, where the error bars overlap significantly less than those in Fig. 10. However, this representation does not give the same degree of separation as that obtained from the nonlinear representation.

While the results obtained from the sparsity assessment may not have been decisive they can be used to create a more detailed representation of the original nature. Fig. 12 gives a 2D state diagram of the response of λ for the sparse hybrid filter plotted against that of the nonlinear hybrid filter. In this case, the values of λ were reversed with $(0, 0)$ indicating a purely linear signal and $(1, 1)$ a nonlinear and sparse signal. The plot originates at $(0, 0.5)$ and shows the evolution of the mixing parameters over 50 seconds of data. These results show that by combining the two mixing parameters there is a clear difference between the nature of both the coma and QBD data.

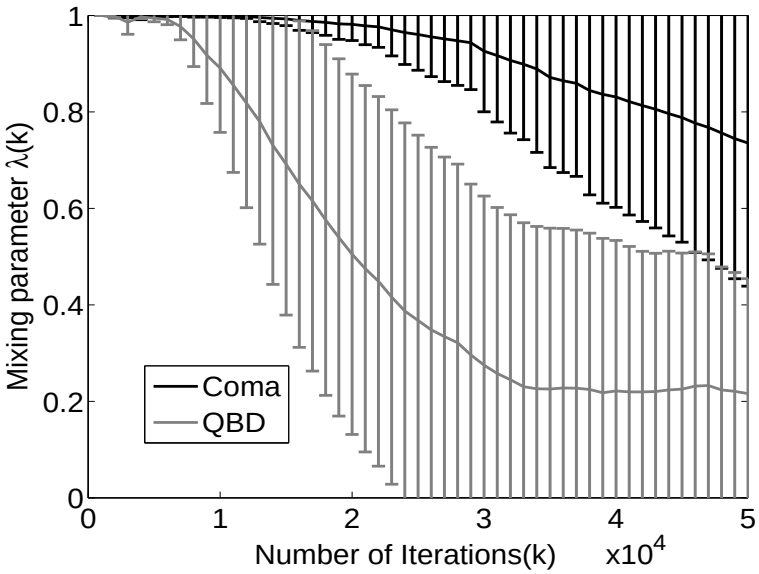

Figure 11: The evolution of the average mixing parameter $\lambda(k)$ for signal sparsity detection, for patients in different brain states, with corresponding standard deviation error bars for 15 coma patients, 15 QBD patients. $\lambda = 1$ corresponds to linear subfilter.

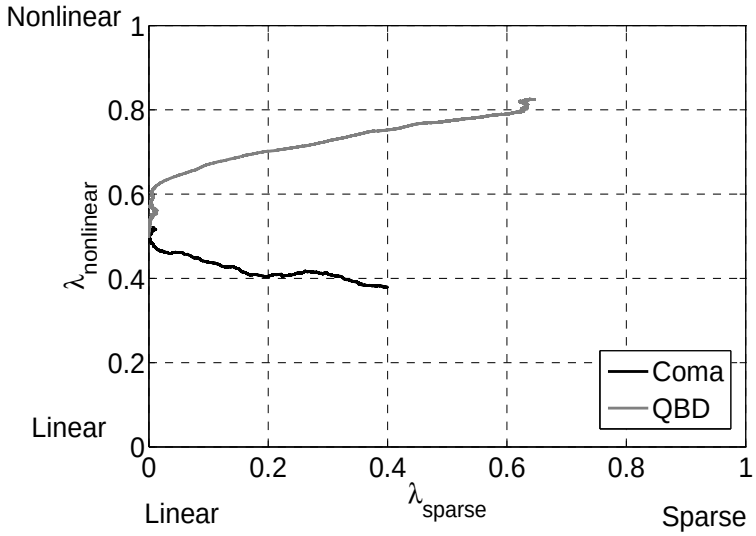

Figure 12: Comparison of the evolution of the mixing parameters for the identification of nonlinearity and sparsity.

4.1. Analysis of Complex EEG Data

When processing the complex valued signals obtained from the combination of Fp1 + $\jmath$Fp2, it was found that in this case both the coma and QBD patients EEG recordings were predominantly linear in nature. However, as previously discussed in Section 2.2, when processing in the complex domain there are distinct differences in characteristics in $\mathbb{C}$ from those in the real domain $\mathbb{R}$. Whilst both signals may be linear in nature, we next consider whether there are differences in the circularity of the signals. To this end the hybrid filter from Section 2.2.1 was implemented. The step size used for the adaptation of λ was 0.3 and the initial value of $\lambda(0) = 1$. The learning rate of the subfilter trained by the CLMS was 0.01 and the learning rate of the ACLMS trained subfilter was 0.01. Simulation results with and without the noisiest data sets are shown in Fig. 13 and Fig. 14 respectively. As previously by design, the mixing parameter $\lambda(k)$ varies between 0 and 1, with a value of λ towards 1 suggesting the signal has a strongly circular nature, and λ towards 0 suggesting the signal is noncircular in nature. From the simulation result of all 34 (17 coma, 17 QBD) patients and the 30 (15 coma, 15 QBD) least noisy recordings, it can be seen that EEG signals of the QBD patients exhibit a more noncircular nature than those of the coma patients.

5. Conclusion

We have proposed nonlinearity analysis of EEG signals as a potential tool for brain consciousness state identification and illustrated how the hybrid filter can be used for this purpose. By monitoring the evolution of the mixing parameter within a hybrid filter, it has been possible to gain insight into the fundamental signal nature, including nonlinearity (in both $\mathbb{R}$ and $\mathbb{C}$), sparsity and complex circularity. Simulation results show great potential of the methodology and its application in signal nonlinearity tracking. Thus, this technique provides a robust feature to determine brain activities and has great potential in the development of a noninvasive test for QBD.

References

[1] H. K. Beecher, A definition of irreversible coma. Report of the ad hoc committee of the Harvard Medical School to examine the definition of brain death., The Journal of the Americal Medical Association 205 (1968) 337–340.

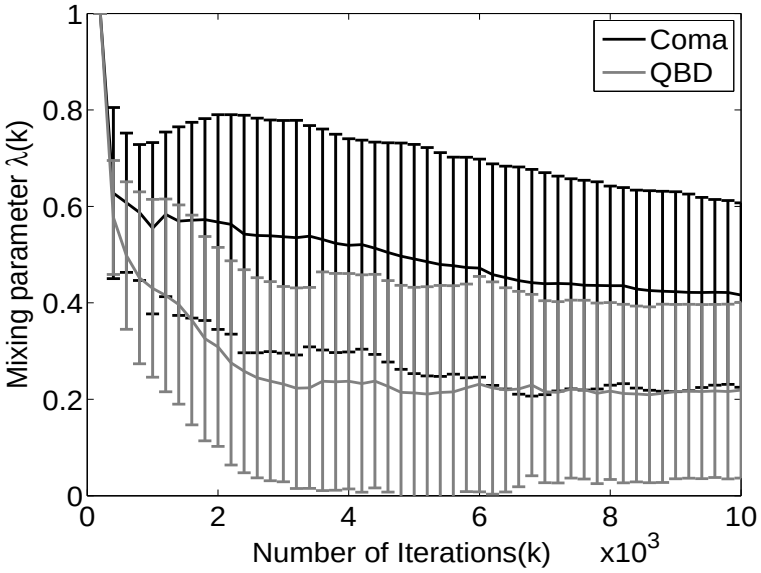

Figure 13: The evolution of the average mixing parameter $\lambda(k)$ for signal circularity detection with corresponding standard deviation error bars for 17 coma patients, 17 QBD patients. $\lambda = 1$ corresponds to circular subfilter.

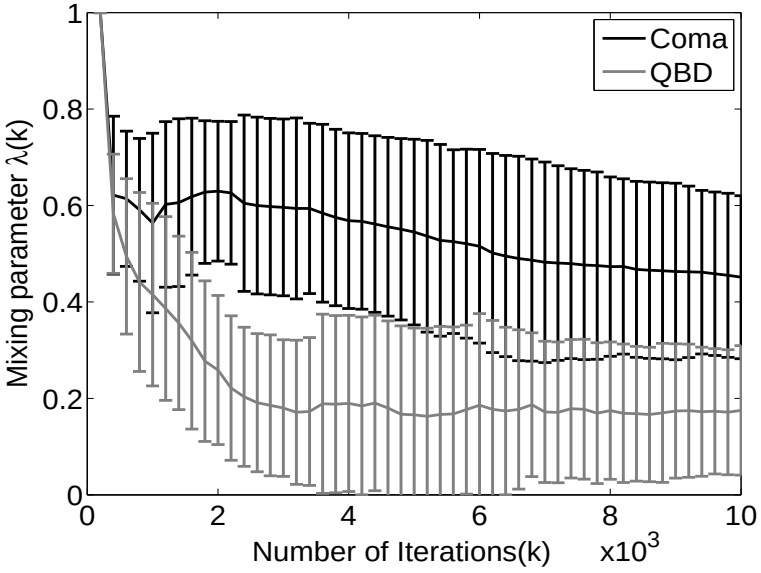

Figure 14: The evolution of the average mixing parameter $\lambda(k)$ for signal circularity detection with corresponding standard deviation error bars for 15 coma patients, 15 QBD patients. $\lambda = 1$ corresponds to circular subfilter.

[2] E. Wijdicks, Brain death worldwide: Accepted fact but no global consensus in diagnostic criteria, Neurology 58 (2002) 20–25.

[3] K. Takeuchi, H. Takeshita, K. Takakura, Y. Shimazono, H. Handa, F. Gotoh, S. Manaka, T. Shiogai, Evolution of criteria for determination of brain death in japan, Acta Neurochirurgica 87 (1987) 93–98.

[4] D. P. Mandic, M. Golz, A. Kuh, D. Obradovic, T. Tanaka (Eds.), Signal Processing Techniques for Knowledge Extraction and Information Fusion, Springer, 2008.

[5] A. Paolin, A. Manuali, F. D. Paola, F. Boccaletto, P. Caputo, R. Zanata, G. P. Bardin, G. Simini, Reliability in diagnosis of brain death, Intensive Care Med. 21 (1995) 657–662.

[6] J. Cao, Analysis of the quasi-brain-death EEG data based on a robust ICA approach, in: Proceedings International Conference on Knowledge-Based & Intelligent Information & Engineering Systems (Lecture Notes in A.I.), volume 4253, pp. 1240–1247.

[7] C. J. Stam, T. Woerkom, W. S. Pritchard, Use of non-linear EEG measures to characterize EEG changes during mental activity, Electroencephalography and Clinical Neurophysiology 99 (1996) 214–224.

[8] L. Li, Y. Saito, D. Looney, T. Tanaka, J. Cao, D. Mandic, Data fusion via fission for the analysis of brain death, in: P. Angelov, D. Filev, N. Kasabov (Eds.), Evolving Intelligent Systems: Methods, Learning and Applications, John Wiley, 2008, pp. 279–320.

[9] B. Boashash, Time Frequency Signal Analysis and Processing: A Comprehensive Reference, Elsevier Science, 2003.

[10] J. Bhattacharya, H. Petsche, Phase synchrony analysis of EEG during music perception reveals changes in functional connectivity due to musical expertise, Signal Processing 85 (2005) 2161–2177.

[11] G. C. Carter, Coherence and Time Delay Estimation, IEEE Press, 1993.

[12] H. Kantz, T. Schreiber, Nonlinear time series analysis Cambridge nonlinear science series, Cambridge University Press, 1997.

[13] T. Gautama, D. P. Mandic, M. M. Van Hulle, Indications of nonlinear structures in brain electrical activity, Phys. Rev. E 67 (2003) 046204.

[14] J. Arenas-Garcia, A. R. Fiqueiras-Vidal, A. H. Sayed, Mean-square performance of a convex combination of two adaptive filters, IEEE Transactions on Siganl Processing 51 (2006) 1078–1090.

[15] B. Jelfs, S. Javidi, P. Vayanos, D. Mandic, Characterisation of signal modality: Exploiting nonlinearity in machine learning and signal processing, Journal of Signal Processing Systems 61 (2010) 105– 115.

[16] T. Gautama, D. P. Mandic, M. Van Hulle, The delay vector variance method for detecting determinism and nonlinearity in time series, Physica D: Nonlinear Phenomena 190 (2004) 167– 76.

[17] D. Looney, C. Park, P. Kidmose, M. Ungstrup, D. P. Mandic, Measuring phase synchrony using complex extensions of EMD, in: Proceedings IEEE 15th Workshop on Statistical Signal Processing (SSP2009), pp. 49–52.

[18] S. Javidi, D. P. Mandic, A. Cichocki, Complex blind source extraction from noisy mixtures using second order statistics, IEEE Transactions on Circuits and System I (2010).

[19] B. Widrow, S. Stearns, Adaptive Signal Processing, Prentice-Hall, 1985.

[20] D. P. Mandic, NNGD algorithm for neural adaptive filters, Electronics Letters 39 (2000) 845–846.

[21] K. Narendra, K. Parthasarathy, Identification and control of dynamical systems using neural networks, IEEE Transactions on Neural Networks 1 (1990) 4–27.

[22] R. K. Martin, W. A. Sethares, R. C. Williamson, C. R. Johnson, Jr., Exploiting sparsity in adaptive filters, IEEE Transactions on Signal Processing 50 (2002) 1883–1894.

[23] P. J. Schreier, L. L. Scharf, C. T. Mullis, Detection and estimation of improper complex random signals, IEEE Transactions on Information Theory 51 (2005) 306–312.

[24] B. Picinbono, On circularity, IEEE Transactions on Signal Processing 42 (1994) 3473–3482.

[25] P. Schreier, L. Scharf, Second-order analysis of improper complex random vectors and processes, IEEE Transactions on Signal Processing 51 (2003) 714–725.

[26] B. Widrow, J. McCool, M. Ball, The complex LMS algorithm, Proceedings of the IEEE 63 (1975) 719–720.

[27] R. Schober, W. H. Gerstacker, L. H.-J. Lampe, A widely linear LMS algorithm for MAI suppression for DS-CDMA, in: IEEE International Conference on Communications, volume 4, pp. 2520–2525.

[28] S. Javidi, M. Pedzisz, S. L. Goh, D. P. Mandic, The augmented complex least mean square algorithm with application to adaptive prediction problems, in: Proceedings of the IAPR Workshop on Cognitive Information Processing, pp. 54–57.

[29] A. Rakotomamonjy, Analysis of SVM regression bounds for variable ranking, Neurocomputing 70 (2007) 1489–1501.

[30] I. T. Jolliffe (Ed.), Principal Component Analysis, Springer, 2002.